

## LOW GAIN ROBUST VISUAL SERVOING WITH BOUNDED TRACKING ERRORS

**P. Zanne** \* **G. Morel** \*\* **F. Plestan** \*\*\*

\* *LSIIT - GRAViR, Université Strasbourg 1 - CNRS, 67400 Illkirch, France, Philippe.Zanne@ensps.u-strasbg.fr*

\*\* *LRP, Université Paris 6 - CNRS, 78400 Vélizy, France, Morel@robot.uvsq.fr*

\*\*\* *IRCCyN, ECN - CNRS, 44321 Nantes, France, Franck.Plestan@irccyn.ec-nantes.fr*

**Abstract:** This paper focuses on the design of robust vision based control of a 2-DOF planar manipulator. The controller is expressed in the image space, where the system can be modeled as a pure integrator with a nonlinear matrix gain. It involves a simple proportional controller with a feedforward velocity input. Robustness is provided by the guarantee of a bounded tracking error, thanks to the online computation on the desired velocity along the trajectory. The approach is both formally proven and experimentally validated on a lab apparatus. *Copyright ©2002 IFAC*

**Keywords:** Robust control, robot vision.

### 1. INTRODUCTION

A major concern in the design of vision based control of robots is the robustness with respect to modeling uncertainties (Hutchinson *et al.*, 1996). Indeed, in this area, practical applications often exhibit uncertainties in both the camera and the robot-environment interaction models. These may significantly affect the overall closed loop behavior.

In the literature, the robustness analysis is focused on the closed loop stability issues. Namely, a conventional control law is used (mostly a proportional controller), and the closed loop stability is proven in the presence of parametric uncertainties (see *e.g.* (Samson *et al.*, 1991; Malis *et al.*, 1999; Kelly, 1996)). Backstepping design has also been used to provide a robust controller for a planar vision based positioning problem in (Zergeroglu *et al.*, 1999), considering also the robustness in terms of closed loop stability.

In this literature, a necessary condition on the stability is the existence of the measured signal: namely, the visually tracked target has to fit in the camera field of view. However, there is no formal guarantee on this particular point. Indeed, the tracking error between the

desired image trajectory and the actual image is not bounded. Thus, even though the desired trajectory can be designed such that it stays within the image limits, large tracking errors may lead the target to actually leave the camera field of view during large motions. To cope with this problem, a sliding mode control approach to visual servoing is proposed in (Zanne *et al.*, 2000), that formally guarantees bounded tracking errors for so-called 3D visual servoing with limited parametric uncertainties. We propose in this paper an alternative control approach, that, by opposition to sliding mode control, does not involve large control gains, nor any switching term in the control input. Rather, the desired velocity is on-line tuned to keep the errors bounded. The advantage of this approach is that, when the uncertainties increase, the robustness is not obtained by increasing the gain, but by slowing down the running velocity along the desired path.

Section 2 details the control approach for a general vision based control problem. The tracking error bounding condition is expressed as a fundamental trade-off between the control gain, the modeling uncertainties, the required precision and the desired velocity. The

computation of this condition is largely inspired from MIMO sliding mode control (Slotine *et al.*, 1991), but it is exploited differently, in a reference velocity adaptation strategy. Section 3 details the model for a particular 2-DOF vision based positioning problem, emphasizing the practical applicability of the approach. Section 4 shows the experimentation of the controller on a planar manipulator.

## 2. CONTROL WITH BOUNDED ERROR

### 2.1 Problem statement

The problem under interest in this section is to propose a provable robust control law with bounded error for vision based tracking. More precisely, the goal is that the state vector  $\mathbf{x} \in \mathbb{R}^n$  (that is an  $n$ -dimensional image feature vector) tracks a desired vector  $\mathbf{x}^*$  with :

$$\forall t > 0, |\mathbf{e}| = |\mathbf{x}(t) - \mathbf{x}^*(t)| \leq \boldsymbol{\varphi} \quad (1)$$

$\boldsymbol{\varphi}$  is a strictly positive  $n$ -dimensional vector and is arbitrarily set by the user. The desired path is given by :

$$\mathbf{x}^* = \mathbf{f}(\alpha) \quad (2)$$

where  $\mathbf{f}$  is a known  $n$ -dimensional vector function describing desired geometrical path, and  $0 \leq \alpha \leq 1$  a scalar parameter. It shall be noticed that the time variation of  $\alpha$  is not a priori known. Rather it is computed so as to respect tracking error bounding constraints, in the presence of bounded uncertainties on the system. Denoting  $\frac{\partial \mathbf{f}}{\partial \alpha}^+$  the right derivative of  $\mathbf{f}$ , the desired state velocity is derived by :

$$\dot{\mathbf{x}}^* = \begin{cases} \dot{\alpha} \frac{\partial \mathbf{f}}{\partial \alpha}^+ & \text{if } \alpha < 1 \\ 0 & \text{if } \alpha = 1 \end{cases} \quad (3)$$

Note that the progression along the desired trajectory is characterized by the condition  $\frac{d\alpha}{dt} > 0$ .

### 2.2 Control design

Our approach (fig.1) involves at the lowest level a conventional fixed gain controller, and, at a higher level, an on-line computation of the desired velocity. In the design of the low level controller, the following model is used to describe the system dynamics :

$$\dot{\mathbf{x}} = \mathbf{J}\mathbf{u} \quad (4)$$

where  $\mathbf{J} \in \mathbb{R}^{n \times n}$  is the so-called image jacobian and  $\mathbf{u} \in \mathbb{R}^n$  is the control input representing the robot velocity. This system is known via an estimated model:

$$\dot{\hat{\mathbf{x}}} = \hat{\mathbf{J}}\mathbf{u} \quad (5)$$

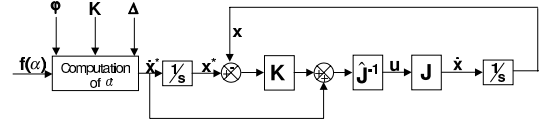


Fig. 1. Control scheme

The proposed control law is :

$$\mathbf{u} = \hat{\mathbf{J}}^{-1} (\mathbf{K}\mathbf{e} + \dot{\mathbf{x}}^*) \quad (6)$$

where  $\mathbf{K} = \text{diag}(\mathbf{k})$  is built from the strictly positive elements of a  $n$ -dimensional gain vector  $\mathbf{k}$ , ( $\forall i, \mathbf{K}_{ii} = \mathbf{k}_i, \mathbf{K}_{ij} = 0, i \neq j$ ). The desired velocity  $\dot{\mathbf{x}}^*$  used as feedforward input is computed from  $\dot{\alpha}$  using Equation (3) and  $\dot{\alpha}$  is given by :

$$\dot{\alpha} = \min_{i \in 1 \dots n} \frac{\sum_{j=1}^n [(\mathbf{I}_n - \Delta)]_{ij} \varphi_j \mathbf{k}_j}{\sum_{j=1}^n \Delta_{ij} \left| \frac{\partial \mathbf{f}}{\partial \alpha}^+ \right|_j} \quad (7)$$

where  $\Delta$  is a  $n \times n$  matrix bounding the parametric uncertainties of the system, such that :

$$\forall i, j \in 1 \dots n, \Delta_{ij} > |\mathbf{D}_{ij}| \quad (8)$$

where  $\mathbf{D}$  is defined by  $\mathbf{D} \triangleq \mathbf{J}\hat{\mathbf{J}}^{-1} - \mathbf{I}_n$ .

*Proposition 1.* If the hypotheses

- $\mathbf{H}_1$   $\hat{\mathbf{J}}$  is of full rank and  $\mathbf{J}\hat{\mathbf{J}}^{-1}$  is definite-positive,
- $\mathbf{H}_2$  At  $t = 0, \mathbf{x}(0) = \mathbf{x}^*(0)$ ,
- $\mathbf{H}_3$  The matrix  $\Delta$  verifies

$$\text{for } i \in 1 \dots n, \sum_{j=1}^n [(\mathbf{I}_n - \Delta)]_{ij} \varphi_j \mathbf{k}_j > 0 \quad (9)$$

are fulfilled, then the system (4) under the control law (6) and (7) is stable in presence on parameters uncertainties bounded by  $\Delta$  and satisfies the bounding condition (1).  $\blacksquare$

The closed loop behavior with the control law (6) is:

$$\begin{aligned} \dot{\mathbf{e}} &= \dot{\mathbf{x}}^* - \mathbf{J}\hat{\mathbf{J}}^{-1} (\mathbf{K}\mathbf{e} + \dot{\mathbf{x}}^*) \\ &= -\mathbf{D}\dot{\mathbf{x}}^* - (\mathbf{D} + \mathbf{I}_n)\mathbf{K}\mathbf{e} \end{aligned} \quad (10)$$

Assumption  $\mathbf{H}_1$  guarantees that the system is non singular and is stable in closed-loop with the low level controller. Without any modeling errors, (*i.e.*  $\hat{\mathbf{J}} = \mathbf{J}$ ), the exponential convergence of each component  $e_i$  of  $\mathbf{e}$  towards 0 is obtained, with a convergence rate tuned by  $\mathbf{k}_i$ .

Assumption  $\mathbf{H}_2$  is not restrictive, since it is always possible to compute a desired trajectory from an initial configuration  $\mathbf{x}(0)$ .

Assumption  $\mathbf{H}_3$  means that the uncertainties cannot be too large to guarantee a bounded tracking error. If one sets for  $i \in 1 \dots n, \mathbf{k}_i = k > 0$  and  $\varphi_i = \phi > 0$ , *i.e.* if the same closed-loop dynamics and the same precision is

required for all the components of  $\mathbf{e}$ , then, Assumption  $\mathbf{H}_3$  is equivalent to:

$$\text{for } i \in 1 \cdots n, \sum_{j=1}^n \Delta_{ij} < 1 \quad (11)$$

Note that if,  $\sum_{j=1}^n \Delta_{ij} \left| \frac{\partial \mathbf{f}}{\partial \alpha} \right|_j = 0$ , for  $i \in 1 \cdots n$ , then any positive choice of  $\dot{\alpha}$  satisfies the bounding condition. In this case,  $\dot{\alpha}$  can be chosen arbitrarily, to a value  $\dot{\alpha}_0$  fixed in advance. ■

### 2.3 Proof of Proposition 1

For the proof of Proposition 1, it is shown that  $\forall t \geq 0$ , for  $i \in 1 \cdots n$ ,  $|\mathbf{e}_i| < \varphi_i$ .

According to Assumption  $\mathbf{H}_2$ , and since states vectors  $\mathbf{x}$  and  $\mathbf{x}^*$  are continuous functions :

$$\exists t_0 \mid \forall 0 \leq t < t_0, i \in 1 \cdots n, |\mathbf{e}_i| \leq \varphi_i \quad (12)$$

which means that the bounding condition is respected at least until a given time  $t_0$ .

Assume that, at a given time  $t_0$ , at least one of components  $\mathbf{e}_i$  of  $\mathbf{e}$  reaches its bound  $\varphi_i$  (that is  $|\mathbf{e}_i| = \varphi_i$  and  $\forall j \neq i |\mathbf{e}_j| \leq \varphi_j$ ). From the definition of  $\dot{\alpha}$  (Eq. 7), one gets :

$$\forall i \in 1 \cdots n, \dot{\alpha} \sum_{j=1}^n \Delta_{ij} \left| \frac{\partial \mathbf{f}}{\partial \alpha} \right|_j \leq \sum_{j=1}^n [(\mathbf{I}_n - \Delta)]_{ij} \varphi_j \mathbf{k}_j \quad (13)$$

According to Assumption  $\mathbf{H}_3$ ,  $\dot{\alpha} > 0$ . Equation (13) implies :

$$(1 - \Delta_{ii}) \mathbf{k}_i \varphi_i \geq \sum_{j=1}^n \Delta_{ij} |\dot{\mathbf{x}}_j^*| + \sum_{j=1, j \neq i}^n \Delta_{ij} \mathbf{k}_j \varphi_j \quad (14)$$

Moreover according to Equation (8) and since it was assumed that at  $t = t_0$   $|\mathbf{e}_i| = \varphi_i$  and  $\forall j \neq i |\mathbf{e}_j| \leq \varphi_j$ , one has :

$$\begin{aligned} (1 + \mathbf{D}_{ii}) \mathbf{k}_i |\mathbf{e}_i| &\geq (1 - \Delta_{ii}) \mathbf{k}_i \varphi_i \\ -\text{sgn}(\mathbf{e}_i) \sum_{j=1}^n \mathbf{D}_{ij} \dot{\mathbf{x}}_j^* &\leq \sum_{j=1}^n \Delta_{ij} |\dot{\mathbf{x}}_j^*| \\ -\text{sgn}(\mathbf{e}_i) \sum_{j=1, j \neq i}^n \mathbf{D}_{ij} \mathbf{k}_j \varphi_j &\leq \sum_{j=1, j \neq i}^n \Delta_{ij} \mathbf{k}_j \varphi_j \end{aligned} \quad (15)$$

Combining Equations (14) and (15), one gets :

$$(1 + \mathbf{D}_{ii}) \mathbf{k}_i |\mathbf{e}_i| \geq -\text{sgn}(\mathbf{e}_i) \left( \sum_{j=1}^n \mathbf{D}_{ij} \dot{\mathbf{x}}_j^* + \sum_{j=1, j \neq i}^n \mathbf{D}_{ij} \mathbf{k}_j \varphi_j \right)$$

then :

$$-\text{sgn}(\mathbf{e}_i) \sum_{j=1}^n \left[ \mathbf{D}_{ij} \dot{\mathbf{x}}_j^* + (\mathbf{D} + \mathbf{I}_n)_{ij} \mathbf{k}_j \varphi_j \right] \leq 0$$

We deduce :

$$\text{sgn}(\mathbf{e}_i) \dot{\mathbf{e}}_i \leq 0 \quad (16)$$

To summarize, if at the given time  $t_0$ , the bound  $\varphi_i$  is reached ( $|\mathbf{e}_i| = \varphi_i$ ), then the tracking error  $|\mathbf{e}_i|$  does not increase. Thus Equation (16) combining with Equation (12) ensures that  $|\mathbf{e}_i| > \varphi_i$ , *i.e.* :

$$\forall t > 0, \forall i \in 1 \cdots n, |\mathbf{e}_i| \leq \varphi_i \quad (17)$$

## 3. MODEL OF THE MANIPULATOR

The system under interest in this paper is a planar manipulator with two perpendicular translation axis. (see Figures 2 and 3) The camera is placed at a fixed position with respect to the robot base.

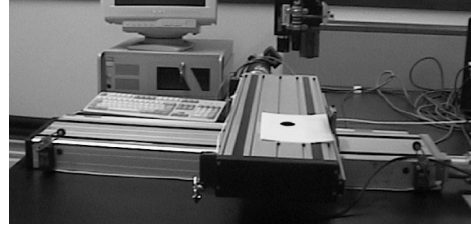


Fig. 2. Photo of the robot-camera system

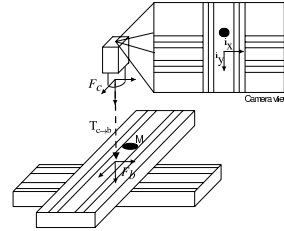


Fig. 3. Schematic representation of the robot-camera system

### 3.1 Real system model

The target mounted on the robot consists of a simple point  $M$ , which coordinates are denoted  $({}^b x, {}^b y, {}^b z)^T$  in the robot base frame  ${}_b$ , and  $({}^c x, {}^c y, {}^c z)^T$  in the camera frame  ${}_c$ . Finally, let  $\mathbf{x} = ({}^i x, {}^i y)^T$  denote the coordinates of  $M$  in the image. The goal of this work is to control the position of a target point  $M$  by tracking a trajectory defined in the image, *i.e.* to control the coordinates  $\mathbf{x}$ . By a classical way, the velocities of the projection of  $M$  in the image are:

$$\dot{\mathbf{x}} = \underbrace{\begin{pmatrix} \frac{g_1}{c_z} & 0 & -\frac{i_x}{c_z} \\ 0 & \frac{g_2}{c_z} & -\frac{i_y}{c_z} \end{pmatrix}}_{\mathbf{J}_i} \begin{pmatrix} {}^c \dot{x} \\ {}^c \dot{y} \\ {}^c \dot{z} \end{pmatrix} \quad (18)$$

with  $g_1$  and  $g_2$  camera intrinsic parameters. As the camera is fixed with respect to the robot base, the relation between the velocities of  $M$  in the camera frame and the base frame is:

$$\begin{pmatrix} {}^c\dot{x} \\ {}^c\dot{y} \\ {}^c\dot{z} \end{pmatrix} = \underbrace{\begin{pmatrix} r_{11} & r_{12} & r_{13} \\ r_{21} & r_{22} & r_{23} \\ r_{31} & r_{32} & r_{33} \end{pmatrix}}_{\mathbf{R}_{cb}} \begin{pmatrix} {}^b\dot{x} \\ {}^b\dot{y} \\ {}^b\dot{z} \end{pmatrix} \quad (19)$$

where  $\mathbf{R}_{cb}$  is the fixed rotation matrix from  $c$  to  $b$ . The closed loop bandwidth of the joint velocity loops is very high as compared to the external visual loop one. Then, high order dynamics is neglected and the system is described as a pure integrator. Furthermore, as the  ${}^b\dot{x}$ -axis (resp.  ${}^b\dot{y}$ -axis) coincide with the first (resp. second) robot axis, one gets :

$$\begin{pmatrix} {}^b\dot{x} \\ {}^b\dot{y} \\ {}^b\dot{z} \end{pmatrix} = \underbrace{\begin{pmatrix} b_x & 0 \\ 0 & b_y \\ 0 & 0 \end{pmatrix}}_{\mathbf{B}} \mathbf{u} \quad (20)$$

Where  $\mathbf{u} = (u_x \ u_y)^T$  is the input voltage. Then, with  $\mathbf{J} = \mathbf{J}_i \mathbf{R}_{cb} \mathbf{B}$ , the planar manipulator can be described by Equation (4).

### 3.2 Estimated model

The following hypotheses are stated to identify the matrix composing  $\mathbf{J}$  in (4). In the practical experiment, the camera has been manually placed such that the optical axis is colinear to the  $z$ -axis of the base robot frame. Consequently, in the estimated model,  ${}^c\hat{z} \equiv \hat{d}$  is the estimated distance between the camera and the target and is supposed constant,  ${}^c\dot{z} = 0$ . Then, one gets:

$$\hat{\mathbf{J}}_i = \begin{pmatrix} \frac{\hat{g}_1}{\hat{d}} & 0 & -\frac{i_x}{\hat{d}} \\ 0 & \frac{\hat{g}_2}{\hat{d}} & -\frac{i_y}{\hat{d}} \end{pmatrix} \quad (21)$$

where  $\hat{g}_1$  and  $\hat{g}_2$  are the estimated intrinsic camera parameters. Furthermore, the knowledge of the actuators allows to estimate the parameters of  $\mathbf{B}$ , and the camera is supposed to be fixed such that the  $c$ -axis are colinear to the  $b$ -axis:

$$\hat{\mathbf{B}} = \begin{pmatrix} \hat{b}_x & 0 \\ 0 & \hat{b}_y \\ 0 & 0 \end{pmatrix} \text{ and } \hat{\mathbf{R}}_{cb} = \mathbf{I}_3 \quad (22)$$

Then, the estimated system from which the control law is designed is  $\dot{\mathbf{x}} = \hat{\mathbf{J}}\mathbf{u} = \hat{\mathbf{J}}_i \hat{\mathbf{R}}_{cb} \hat{\mathbf{B}}\mathbf{u}$ .

### 3.3 Bounding uncertainties

In order to implement the proposed control strategy, lets compute  $\Delta$  bounding  $\mathbf{D}$  given by:

$$\begin{aligned} \mathbf{D} &= \mathbf{J}\hat{\mathbf{J}}^{-1} - \mathbf{I}_2 \\ &= \begin{pmatrix} \frac{\hat{d}}{c_z} \frac{b_x r_{11} g_1}{\hat{g}_1 \hat{b}_x} - 1 & \frac{\hat{d}}{c_z} \frac{b_y r_{12} g_1}{\hat{g}_2 \hat{b}_y} \\ \frac{\hat{d}}{c_z} \frac{b_x r_{21} g_2}{\hat{g}_1 \hat{b}_x} & \frac{\hat{d}}{c_z} \frac{b_y r_{22} g_2}{\hat{g}_2 \hat{b}_y} - 1 \end{pmatrix} \\ &\quad - \frac{\hat{d}}{c_z} \begin{pmatrix} \frac{b_x r_{31} i_x}{\hat{g}_1 \hat{b}_x} & \frac{b_y r_{32} i_x}{\hat{g}_2 \hat{b}_y} \\ \frac{b_x r_{31} i_y}{\hat{g}_1 \hat{b}_x} & \frac{b_y r_{32} i_y}{\hat{g}_2 \hat{b}_y} \end{pmatrix} \end{aligned} \quad (23)$$

First, the uncertainties on constant scalar parameters are supposed to be bounded by:

$$\begin{cases} \frac{1}{\beta_g} \leq \left( \frac{\hat{g}_1}{g_1}, \frac{\hat{g}_2}{g_2} \right) \leq \beta_g & \frac{1}{\beta_z} \leq \frac{\hat{d}}{c_z} \leq \beta_z \\ \frac{1}{\beta_b} \leq \left( \frac{\hat{b}_x}{b_x}, \frac{\hat{b}_y}{b_y} \right) \leq \beta_b \end{cases} \quad (24)$$

where  $\beta_g$ ,  $\beta_b$  and  $\beta_z$  are the user designed bounds on the relative uncertainties for the intrinsic camera parameters, the low level velocity loop gains, and the distance from the camera to the robot base frame, respectively. The elements of  $\mathbf{R}_{c \rightarrow b}$  have to be bounded.  $\mathbf{R}_{c \rightarrow b}$  is represented by an angle  $\theta$  (see Figure 3) around a unitary vector  $\mathbf{v}$ . We have  $\mathbf{R}_{c \rightarrow b} = \mathbf{I}_3 + \sin \theta [\mathbf{v}]_{\times} + (1 - \cos \theta) [\mathbf{v}]_{\times}^2$ , with  $[\mathbf{v}]_{\times}$  the skew symmetric matrix associated with the vector  $\mathbf{v}$ , such that  $\forall \mathbf{a}, \mathbf{v} \times \mathbf{a} = [\mathbf{v}]_{\times} \mathbf{a}$ . Then,  $r_{ii} = (1 - \cos \theta) v_i^2 + \cos \theta$  and  $r_{ij} = \pm \sin \theta v_k + (1 - \cos \theta) v_i v_j$  for  $i \neq j \neq k$ . Assuming that  $|\theta| \leq \theta_m$ , one gets

$$|r_{ii}| \leq 1 \quad (25)$$

$$|r_{ij}| \leq \gamma_m = \sin \theta_m + \frac{\sqrt{2}}{2} (1 - \cos \theta_m), \quad i \neq j. \quad (26)$$

Combining these last relations with (23) and (24), the matrix  $|\mathbf{D}|$  is bounded by:

$$\begin{aligned} \Delta &= \begin{pmatrix} \beta_b \beta_g \beta_z - 1 & \beta_b \beta_g \beta_z \frac{\hat{g}_1}{\hat{g}_2} \gamma_m \\ \beta_b \beta_g \beta_z \frac{\hat{g}_2}{\hat{g}_1} \gamma_m & \beta_b \beta_g \beta_z - 1 \end{pmatrix} \\ &\quad + \beta_g \beta_z \gamma_m \begin{pmatrix} \frac{|i_x|}{\hat{g}_1} & \frac{|i_x|}{\hat{g}_2} \\ \frac{|i_y|}{\hat{g}_1} & \frac{|i_y|}{\hat{g}_2} \end{pmatrix} \end{aligned} \quad (27)$$

## 4. EXPERIMENTS

This section describes the application of the previous sections results to a simple 2-DOF visual servoing system. The task consists in tracking a desired trajectory in the image space with a weakly calibrated system such that the tracked object follows its desired

image trajectory with a bounded tracking error. The uncertainties arise from the intrinsic parameters of the camera, the linear gain of the low level velocity servo loops, and the position of the camera in the robot frame.

Experiments were conducted in our laboratory using a 2 axis planar robot (see Figure 1). The estimated parameters for this system are given in Table 1. Practically, the orientation of the camera has been

Parameter	Estimated Value	Unit
$\hat{\theta}$	0	rad
$\hat{g}_1$	768.07	pixels
$\hat{g}_2$	387.62	pixels
$\hat{b}_x = \hat{b}_y$	0.056	(m/s)/V
$\hat{d}_3$	0.215	m

Table 1. Estimated parameters

set with a rough inclinometer. The parameter  $d$  is estimated with a simple ruler. The intrinsic camera parameters are the ones given by the camera constructor. The gains  $b_x$  and  $b_y$  are estimated from the tachymeter gain and the transmission gear ratio. Table 2 gives the maximum amount of uncertainty assumed for the experiment. In this table, the parameter  $\gamma_m$  is directly

Bound	Value	Unit
$\theta_m$	5	deg
$\gamma_m$	0.0898	
$\beta_g$	1.2	
$\beta_b$	1.01	
$\beta_z$	1.1	

Table 2. Parametric uncertainty bounds

computed from  $\theta_m$  using Equation (26). With these parametric uncertainty bounds,  $\Delta$  is given by:

$$\Delta = \begin{pmatrix} 0.333 & 0.237 \\ 0.061 & 0.333 \end{pmatrix} + 0.11 \begin{pmatrix} \frac{|i_x|}{768} & \frac{|i_x|}{387} \\ \frac{|i_y|}{768} & \frac{|i_y|}{387} \end{pmatrix}$$

The desired geometrical path is described by Equation :

$$\forall \alpha \in [\alpha_1; \alpha_2] \begin{cases} i_{x^*} = a_1 \alpha + a_2 \\ i_{y^*} = b_1 \alpha + b_2 \end{cases} \quad (28)$$

where

$\alpha_1$	$\alpha_2$	$a_1$	$a_2$	$b_1$	$b_2$
0	0.142	1780	320	-41	120
0.142	0.438	1780	840	0	60
0.438	0.506	0	60	1780	-720
0.506	0.798	1780	-840	0	180
0.798	0.854	0	580	-1780	1600
0.854	1	-1780	2100	274	-154

Table 3. Geometrical path parameters

The tracking error bound is set to  $\varphi_1 = \varphi_2 = 4$  pixels,  $\mathbf{k}_1 = \mathbf{k}_2 = 5s^{-1}$ . As the image coordinates are bounded by  $|i_x| < 320$  and  $|i_y| < 120$ , Equation (11) and Assumption  $\mathbf{H}_3$  are verified:  $\Delta_{11} + \Delta_{12} \leq 0.717$  and

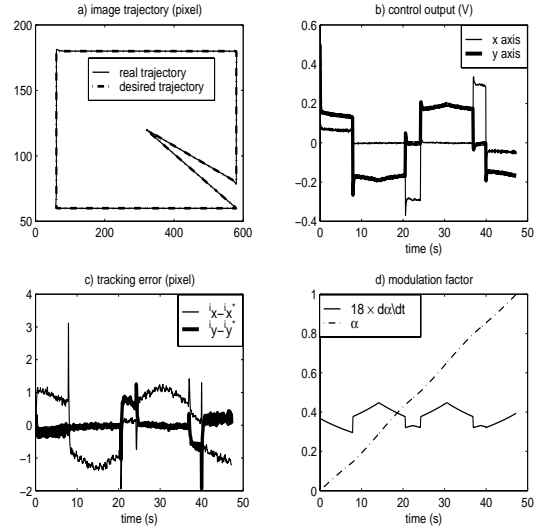


Fig. 4. Experimental results

$\Delta_{21} + \Delta_{22} \leq 0.449$ . The test trajectory involves 6 linear sections in different directions. At the beginning of the experiment, the current image point  $\mathbf{x}$  is placed at the initial desired value  $\mathbf{x}^*$ :  $\mathbf{H}_2$  is verified. From (21) and (22), it is obvious to prove that  $\hat{\mathbf{J}}$  is non singular ; furthermore, viewed the choice of  $\varphi_1 = \varphi_2$  and  $\mathbf{k}_1 = \mathbf{k}_2$  and viewed that  $\mathbf{H}_3$  is fulfilled, then it is easy to verify that  $\mathbf{J}\hat{\mathbf{J}}^{-1} = \mathbf{D} + \mathbf{I}_n$  is definite-positive :  $\mathbf{H}_1$  is verified. Then, by tuning the motion velocity from (7), the tracking error will stay in the bounds defined by  $\varphi_1$  and  $\varphi_2$ .

Figure 4 displays the experimental results. The a) plot displays the real and desired trajectories. From the c) plot, we see the magnitude of the error is smaller than  $\varphi_1$  for  $x$ -axis and  $\varphi_2$  for  $y$ -axis, all over the experiment. The b) plot displays control inputs of the actuators. The d) plot displays the evolution of the parameter  $\alpha$  and an image of the motion velocity variation along the desired trajectory. It shows that its variation is necessary to ensure that the error is bounded and stays in the area stated by the user.

## 5. CONCLUSION

In this paper we have addressed the problem of robust control of robots from visual information in presence of parametric uncertainties. A methodology based on the on line computation of the desired velocity to deal with bounds on the tracking error has been proposed and successfully experimented. Our work is currently focusing on implementation the article results to a 6 D.O.F visual servoing system.

## 6. REFERENCES

Hutchinson S., G.D. Hager, P.I. Corke (1996), A tutorial on visual servo control, *IEEE Transactions on Robotics and Automation*, Vol. 12, 5, pp. 651–670.

- Samson C., B. Espiau, M. Le Borgne (1991), Robot control : the task function approach, in *Oxford science publications*, Clarendon Press.
- Malis E., F. Chaumette, S. Boudet (1999), 2-1/2-D Visual Servoing, *IEEE Transactions on Robotics and Automation*, Vol. 15, 2, pp. 238–250.
- R. Kelly (1996), Robust Asymptotically Stable Visual Servoing of Planar Robots, *IEEE Transactions on Robotics and Automation*, Vol. 12, 5, pp. 759–766
- E. Zergeroglu, D.M. Dawson, M.S.de Queiroz and S. Nagarkatti (1999), Robust Visual-Servo Control of Robot Manipulators in the Presence of Uncertainty, *Proc. IEEE Conference on Decision and Control*, Phoenix, Arizona, pp. 4137–4142.
- Zanne P., G. Morel, F. Plestan (2000), Robust vision based 3D trajectory tracking using sliding mode control, *Proc. IEEE International Conference on Robotics and Automation*, San Fransisco, California.
- Slotine J.J.E., W. Li (1991), Applied nonlinear control, Prentice-Hall International Editions, Englewood Cliffs.